A multicenter numerical integration scheme for polyatomic molecules

A. D. Becke

Department of Chemistry, Queen's University, Kingston, Ontario K7L 3N6, Canada

We propose a simple scheme for decomposition of molecular functions into single-center components. The problem of three-dimensional integration in molecular systems thus reduces to a sum of one-center, atomic-like integrations which are treated using standard numerical techniques in spherical polar coordinates. The resulting method is tested on representative diatomic and polyatomic systems for which we obtain five- or six-figure accuracy using a few thousand integration points per atom.

I. INTRODUCTION

For many decades now, quantum chemists have relied on finite basis-set expansions as their primary computational tool. LCAO (linear combination of atomic orbitals) is currently the only viable general approach to *ab initio* computational chemistry. This dependence on finite basis sets has, however, undesirable consequences. A major part of virtually every quantum chemical publication is devoted to analysis of the basis sets employed in the calculations, reflecting the nagging and ever-present specter of basis-set incompleteness. Moreover, the inevitable discussion of basis-set details is, at least from a fundamental point of view, rather uninteresting.

Attempts have been made in recent years to escape from the conventional LCAO framework. In the special case of *diatomic* molecules, completely numerical, non-basis-set calculations are now possible on discrete two-dimensional meshes in prolate spheroidal coordinates. The first calculations of this numerical type were carried out in 1981 by the present author (see Ref. 1) on first-row diatomic systems in the Hartree–Fock–Slater or $X\alpha$ approximation.[2] Since then, our method has evolved significantly and has recently been applied to dimers as heavy as Cr_2 using various contemporary density functional theories.[3,4] A similar method has also been developed by Pyykkö and co-workers[5] with applications to a great variety of quantum chemical formalisms such as Hartree–Fock, $X\alpha$, MCSCF, and Dirac–Slater.[6] Completely numerical diatomic calculations are admittedly costly, but by now essentially routine. Note, however, that numerical computations are perfectly suited for vector and parallel processing. As parallel computing technology advances, therefore, discrete numerical techniques will become increasingly attractive.

It is our desire to develop a completely numerical, non-basis-set scheme for quantum chemical calculations on polyatomic molecules, in general. No such scheme currently exists (at least in *real* space, but see Ref. 7 for a proposed method in *momentum* space). In the present work, we take an initial step in this direction. Considered here is the fundamental problem of discrete numerical integration in multicenter systems.

Even if the ultimate objective of completely basis-set-free quantum chemistry is not soon realized, the ability to carry out numerical integrations in polyatomic molecules is itself of immediate value. This is due to the increasing importance in quantum chemistry of so-called *density functional* theories, in which exchange and/or correlation energies of many-electron systems are approximated by three-dimensional integrals of local exchange-correlation densities derived from electron gas theory. The power of density functional methods has been aptly demonstrated in recent applications to diatomic, organometallic, and transition metal binuclear complexes in Refs. 4, 8, and 9, respectively, and the interested reader will find general reviews of the theoretical framework in Ref. 10. The reader should appreciate that the exchange-correlation integrals of density functional theories cannot be evaluated analytically, even in an LCAO context, and therein lies the importance of numerical integration algorithms.

In Sec. II, then, we outline the basic philosophy of the present integration scheme, and also discuss its extension to problems beyond the integration problem. Then, in Secs. III and IV, the method is described in detail. In Sec. V, the scheme is tested on the diatomic systems H_2, N_2, and P_2, and on seven representative polyatomic systems of various geometries using integrands of density functional type. Diatomic systems are included for testing purposes because "exact" results for arbitrary integrands are obtainable from our existing numerical diatomic program.[1] Finally, we offer concluding remarks in Sec. VI. We include, also, an Appendix in which the reader will find certain details of secondary importance.

II. GENERAL PHILOSOPHY

We are concerned with three-dimensional molecular integrals of the type

$$I = \int F(\mathbf{r})d^3\mathbf{r}, \tag{1}$$

where $F(\mathbf{r})$ is an arbitrary integrand. These may be approximated by discrete numerical summations of the form

$$I = \sum_i A_i F(\mathbf{r}_i), \tag{2}$$

where the $\mathbf{r}_i$ and A_i are discrete integration points and their respective integration weights whose optimum distribution is the subject of the present work.

In molecules, of course, the integrand $F(\mathbf{r})$ is dominated by cusps at atomic nuclei. Obviously, then, a straightforward

discrete integration in Cartesian coordinates is not recom-
mended, though a marginally successful such scheme has
nevertheless been proposed.[11] Alternatively, standard or-
thogonal *curvilinear* coordinates exist for the special case of
two-center systems[12] and these have been fully exploited in
the previously-cited work of Becke[1] and Pyykkö *et al.*[5] on
diatomic molecules. For systems containing three or more
centers, however, standard multicenter coordinates do not
exist, and we therefore face a difficult problem.

An obvious and popular solution to this multicenter in-
tegration problem involves partitioning of molecular space
into discrete regions or "cells" of simple geometry commen-
surate with the positions of the nuclei, such that straightfor-
ward numerical integration may be carried out within each
region. This cellular approach has been developed to a high
degree of sophistication in the recent work of Boerrigter, te
Velde, and Baerends.[13] Cellular methods require, however,
considerable intuition and input regarding the disposition of
the various regions. A scheme requiring knowledge only of
the positions (and perhaps charges) of the atomic nuclei,
such as proposed in the present communication, would be
somewhat more convenient.

In the context of cellular methods, the work of Bader
and co-workers (see, e.g., Ref. 14 and references therein) is
also relevant. Bader has defined atomic fragments in molec-
ular systems on the basis of the topology of the total electron
density. These atomic fragments have fascinating theoretical
significance and ingenious numerical techniques have been
devised for integrating within them.[15] Though the primary
applications of Bader's formalism are theoretical and inter-
pretative, some of the associated numerical techniques could
conceivably be adopted for general-purpose molecular inte-
gration as well.

We should also acknowledge the method of Ellis and
Painter[16] which has played such an important role in the
development of the Hartree–Fock–Slater molecular struc-
ture program of Baerends and co-workers (see Ref. 17 and
references therein). The method of Ellis and Painter, based
on Diophantine theory,[18] behaves rather poorly as the num-
ber of integration points increases, however, and is therefore
unsuitable for integration of high accuracy. The reader is
referred, e.g., to a comparison with the method of Boerrigter
et al. in Ref. 13.

The approach of the present work is based on a very
simple philosophy. We assume that a *relative weight* func-
tion $w_n(\mathbf{r})$ can be assigned to each nucleus n in the system
such that, for all $\mathbf{r}$,

$$\sum_n w_n(\mathbf{r}) = 1 \tag{3}$$

and such that each $w_n(\mathbf{r})$ has value *unity* in the vicinity of its
own nucleus, but *vanishes* in a continuous and well-behaved
manner near *any other* nucleus. In a sense, then, the system is
divided not into conventional discrete cells, but into *fuzzy,
overlapping, analytically continuous* cells instead. This image
of a "fuzzy" cellular partitioning is not intended merely as a
visual aid, but will, in fact, be implemented quite literally in
Sec. III.

An arbitrary molecular function $F(\mathbf{r})$ may thus be de-

composed into single-center components $F_n(\mathbf{r})$ as follows:

$$F(\mathbf{r}) = \sum_n F_n(\mathbf{r}), \tag{4}$$

where

$$F_n(\mathbf{r}) = w_n(\mathbf{r})F(\mathbf{r}) \tag{5}$$

and the multicenter integration of Eq. (1) therefore reduces
to a sum of *single*-center integrations I_n over each of the
nuclei in the system:

$$I = \sum_n I_n, \tag{6}$$

where

$$I_n = \int F_n(\mathbf{r}) \, d^3\mathbf{r}. \tag{7}$$

If the weight functions $w_n(\mathbf{r})$ are sufficiently well behaved,
as defined more precisely in Sec. III, then each atomic subin-
tegration I_n may be carried out using standard single-center
numerical techniques in spherical polar coordinates.

This philosophy is not, in a general sense, particularly
new. A conceptually similar approach has also been de-
scribed by Boys and Rajagopal.[19] The present work, how-
ever, and particularly the present decomposition scheme,
differs considerably in detail.

Also, we wish to point out that the present decomposi-
tion scheme extends naturally to the problem of solving Pois-
son's equation:

$$\nabla^2 V_{\text{el}}(\mathbf{r}) = -4\pi\rho(\mathbf{r}) \tag{8}$$

for the Coulomb potential $V_{\text{el}}(\mathbf{r})$ due to an electron density
distribution $\rho(\mathbf{r})$. Fully numerical solution of Poisson's
equation, though tractable in diatomic systems as a result of
the work of Becke[1] and Pyykkö *et al.*,[5] is not yet feasible
generally. If, however, the proposed atomic decomposition
scheme is applied to the density distribution $\rho(\mathbf{r})$, then Eq.
(8), being linear, reduces to a set of independent *one*-center
equations, each of which may then be solved using standard
single-center techniques such as spherical harmonic analy-
sis, etc. Fully numerical solution of Poisson's equation, in
combination with a good numerical integration scheme
(such as the scheme proposed here), would allow basis-set-
free computation of molecular Coulomb interaction energies
and matrix elements. We are currently pursuing this prob-
lem and hope to discuss it further in later publications.

III. NUCLEAR WEIGHT FUNCTIONS

We now describe a novel procedure for generating the
nuclear weight functions $w_n(\mathbf{r})$ introduced in Sec. II. We
begin by considering a conventional cellular partitioning of
molecular space into so-called Voronoi polyhedra. Then, we
"soften" the boundaries of the resulting polyhedra to create
the "fuzzy cells" to which we alluded above.

Given an arbitrary distribution of atomic centers in
three-dimensional space, a unique polyhedron may be asso-
ciated with each nucleus by a relatively simple prescription.
Consider, e.g., nucleus i as reference, and construct for every
other nucleus $j \neq i$ the perpendicular bisecting plane of the
vector joining i to j. Clearly, the minimum volume enclosed

by all these bisecting planes is a *polyhedron* containing all points nearer to nucleus i than to any other. These unique polyhedra, one for each i, perfectly fill the space of the molecule and are called Voronoi polyhedra (or Voronoi cells). In the special case of a *periodic* atomic lattice, these are somewhat better known as Wigner–Seitz cells.

Efficient algorithms for the automatic construction of Voronoi polyhedra have been published (see, e.g., Ref. 20 and references therein), but we shall introduce a rather unconventional scheme which is uniquely appropriate for the present purposes.

Our scheme involves the popular two-center coordinate system known as confocal elliptical coordinates (λ,μ,ϕ). The coordinate ϕ denotes angle about the internuclear axis, and coordinates λ and μ are defined by

$$\lambda = \frac{r_1 + r_2}{R_{12}}, \quad \mu = \frac{r_1 - r_2}{R_{12}}, \tag{9}$$

where r_1, r_2, and R_{12} denote distance to nucleus 1, distance to nucleus 2, and the internuclear separation, respectively. The coordinate λ labels ellipsoids of revolution with foci at the positions of the nuclei, and μ similarly labels hyperboloids. Their ranges are indicated below:

$$0 \leqslant \phi \leqslant 2\pi,$$
$$1 \leqslant \lambda < \infty, \tag{10}$$
$$-1 \leqslant \mu \leqslant +1.$$

Notice that the surface $\mu = 0$ corresponds to the perpendicular bisector of the internuclear axis, just as required in the construction of Voronoi polyhedra. Also, we note that $\mu = -1$ corresponds to a semi-infinite ray extending from center 1 along the nuclear axis to infinity, and that $\mu = +1$ corresponds to a similar ray from center 2 to infinity.

Elliptical coordinates furnish a natural and convenient definition of Voronoi polyhedra in an interesting analytical sense. With center i as reference, consider in turn each of the other centers $j \neq i$ and establish elliptical coordinates λ_{ij}, μ_{ij}, and ϕ_{ij} on the foci i and j. Of special interest is the coordinate

$$\mu_{ij} = \frac{r_i - r_j}{R_{ij}}, \tag{11}$$

where r_i and r_j denote distances to nuclei i and j, respectively, and R_{ij} is the internuclear separation. With this hyperboloidal coordinate as argument, consider the step function

$$s(\mu_{ij}) = \begin{cases} 1, & -1 \leqslant \mu_{ij} \leqslant 0 \\ 0, & 0 < \mu_{ij} \leqslant +1 \end{cases} \tag{12}$$

and then, recalling that the surface $\mu_{ij} = 0$ is the perpendicular bisector of R_{ij}, observe that the Voronoi polyhedron on nucleus i is defined by the following simple product:

$$P_i(\mathbf{r}) = \prod_{j \neq i} s(\mu_{ij}). \tag{13}$$

This product, which will hereafter be called a "cell function," has value unity if $\mathbf{r}$ lies inside the cell, and vanishes if $\mathbf{r}$ lies outside.

The above definition of Voronoi cells suggests an obvious generalization. Let us replace the step function of Eq. (12) with an appropriate *continuous* analog, resembling, e.g., the finite-temperature Fermi function of statistical me-

chanics. In other words, let us soften or "smooth out" the step discontinuity at $\mu_{ij} = 0$. The cell functions of Eq. (13) will now, as a consequence, represent *analytically continuous, mutually overlapping* regions, and we thereby create the fuzzy Voronoi polyhedra visualized earlier.

Having thus expanded its original definition to include continuous analogs, we will hereafter refer to $s(\mu_{ij})$ as a "cutoff function" or a "cutoff profile." Possible cutoff profiles are not, of course, unique, but we shall impose the following minimum requirements:

$$s(-1) = 1,$$
$$s(+1) = 0, \tag{14}$$
$$\frac{ds}{d\mu}(-1) = \frac{ds}{d\mu}(+1) = 0. \tag{15}$$

The derivative constraints of Eq. (15) ensure that $s(\mu_{ij})$ does not have nuclear cusps. After considerable experimentation with a variety of possible functional forms, including rational, exponential, and trigonometric forms, we have found a particularly useful representation involving simple polynomials only. We describe this representation below.

Consider, first of all, the related problem of finding an odd function $f(\mu)$ in the interval $-1 \leqslant \mu \leqslant +1$ with the properties

$$f(-1) = -1,$$
$$f(+1) = +1, \tag{16}$$
$$\frac{df}{d\mu}(-1) = \frac{df}{d\mu}(+1) = 0, \tag{17}$$

from which the cutoff function $s(\mu)$ is obtained by the transformation

$$s(\mu) = \tfrac{1}{2}[1 - f(\mu)]. \tag{18}$$

The simplest possible $f(\mu)$ satisfying the above constraints is a two-term polynomial:

$$p(\mu) = \tfrac{3}{2}\mu - \tfrac{1}{2}\mu^3. \tag{19}$$

This simple polynomial varies smoothly between the endpoints -1 and $+1$, but, for reasons discussed momentarily, is not "sharp" enough (i.e., not "step function-like" enough) for our purposes. If, however, we *iterate* as follows:

$$f_1(\mu) = p(\mu),$$
$$f_2(\mu) = p[p(\mu)],$$
$$f_3(\mu) = p\{p[p(\mu)]\}, \ldots, \tag{20}$$

then successively sharper functions may be generated with increasing iteration order k. For extremely large k, in fact, a step function is ultimately evolved.

A useful sequence of cutoff profiles $s_k(\mu)$ is thus generated from the above sequence of $f_k(\mu)$ by Eq. (18):

$$s_k(\mu) = \tfrac{1}{2}[1 - f_k(\mu)]. \tag{21}$$

We face, however, the problem of determining the optimum value of k. It is here that the stipulation "sufficiently well behaved," invoked somewhat vaguely in Sec. II, must be satisfied. If k is too small, then $s_k(\mu_{ij})$ will not sufficiently extinguish the nuclear cusp on center j. If k is too large, on

the other hand, the step function of Eq. (12) is recovered and we revert, therefore, to conventional discrete cells. Our sequence of cutoff profiles is illustrated in Fig. 1 for values of k from 1 to 5. We have found, on the basis of our experience thus far, that the value $k = 3$ is appropriate for general applications. This particular choice has therefore been used in all calculations of the present work, and is convincingly supported by the quality of our results in Sec. V.

The above polynomial cutoff profiles strictly satisfy the constraints of Eq. (14). Therefore, the ith cell function $P_i(\mathbf{r})$, in accordance with the definition of Eq. (13), has value *unity* at nucleus i, but *vanishes* at all other nuclei $j \neq i$ and also on each semi-infinite ray extending from j to infinity along the ij axis. These cell functions are obvious candidates for the nuclear weights $w_n(\mathbf{r})$. In order to satisfy Eq. (3), however, we use the following definition:

$$w_n(\mathbf{r}) = P_n(\mathbf{r}) \Big/ \sum_m P_m(\mathbf{r}), \tag{22}$$

where the summation over m in the denominator includes all nuclei in the system (i.e., $m = n$ as well).

Our description of the atomic decomposition scheme is now essentially complete, insofar, at least, as *homonuclear* systems (i.e., atoms of one kind only) are concerned. In *heteronuclear* systems, though, the scheme would obviously benefit from an ability to accommodate varying atomic sizes. Atomic size adjustments are indeed possible, and have, in fact, been incorporated. We wish to proceed at this time, however, to a description of the single-center atomic subintegrations, and therefore, we defer discussion of atomic size adjustments to the Appendix.

IV. SINGLE-CENTER SUBINTEGRATIONS

Having discussed the atomic decomposition scheme, we now describe our numerical procedure for computing the single-center integrals I_n of Eq. (7). The following description applies independently to each nucleus in the molecule.

If we establish a spherical polar coordinate system (r, ϑ, ϕ) on nucleus n, then the volume integral of the single-center component $F_n(\mathbf{r})$ is given by the familiar expression

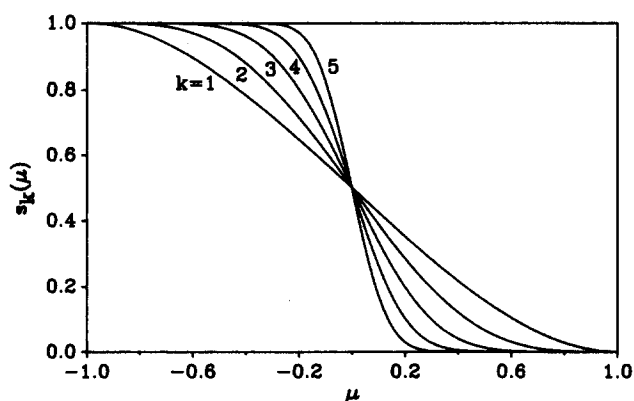$$I_n = \iiint F_n(r, \vartheta, \phi) r^2 \sin \vartheta \, dr \, d\vartheta \, d\phi. \tag{23}$$

This three-dimensional integration may be carried out by treating each of the r, ϑ, and ϕ coordinates independently. There exists, however, a small but impressive literature on Gauss-type quadrature formulas for direct two-dimensional integration on the surface of the unit sphere (see Refs. 21 to 28) and we therefore write

$$I_n = \iint F_n(r, \Omega) r^2 \, dr \, d\Omega, \tag{24}$$

where Ω denotes solid angle. Integration on the surface of the unit sphere and integration over solid angle are, of course, equivalent. In subsequent paragraphs, then, we consider first of all the indicated solid-angle integration and then we discuss the radial part.

Numerical integration on the surface of the unit sphere is a problem of fundamental interest. Following the important early work of McLaren,[21] Stroud,[22] and Sobolev,[23] quadrature formulas of remarkably high order (up to $l = 35$, where all spherical harmonics of order l or less are integrated exactly) have been published by Lebedev[24-27] and by Konyaev.[28] We have coded Lebedev's quadratures of orders 11, 17, and 23 containing 50, 110, and 194 integration points, respectively (Refs. 24 and 25) for the investigations of the present work. The resulting point distributions are invariant with respect to the octahedral group. The point distributions of Konyaev,[28] on the other hand, have icosahedral symmetry.

The reader may wonder if such large angular meshes are really necessary, or, indeed, if they need be even larger. Excessively large meshes as implied by the integration of off-center nuclear cusps are clearly not required. Nevertheless, our cutoff profiles $s(\mu_{ij})$ display significant step-function-like features in internuclear regions, and, as a consequence, moderately large angular meshes are indeed necessary. Our experience thus far indicates that something in the order of 100 or 200 angular points is appropriate for five- or six-figure integration accuracy (see Sec. V).

The radial integrations are performed using standard Gauss–Chebyshev quadrature of the second kind.[29] We prefer Gauss–Chebyshev to the much more popular Gauss–Legendre quadrature because Chebyshev points and weights are given by simple analytical formulas. First, however, the standard Gauss–Chebyshev integration interval $-1 \leqslant x \leqslant +1$ must be mapped into the semi-infinite radial interval $0 \leqslant r < \infty$. This is accomplished by the following coordinate transformation:

$$r = r_m \frac{(1 + x)}{(1 - x)}, \tag{25}$$

where r_m is a parameter corresponding to the midpoint of the integration interval at $x = 0$. This parameter allows adjustment of the radial point distribution to a suitable physical scale. In the present work, r_m is chosen as *half* of the *Bragg–Slater radius* of the respective atom (see Ref. 30 and also the Appendix), except for hydrogen in which case the factor 1/2 is not applied.

The number of radial points on each center is difficult to assign uniquely and depends, of course, on desired precision and on the particular atom in question. Nevertheless, the following empirical rule of thumb appears to provide a rela-

FIG. 1. Cutoff profiles $s_k(\mu)$ of Eq. (21) for $k = 1$ to 5.

tive integration accuracy in the order of 10^{-5}. The hydrogen atom receives an initial quota of 20 radial points, and, thereafter, an additional 5 points are assigned for each additional atomic shell. This rule of thumb assigns, e.g., 25 radial points to the first-row atoms Li to Ne, and 30 points to the second-row atoms Na to Ar, etc. Greater or fewer points are appropriate, of course, if relative integration accuracy greater or less than 10^{-5} is required.

The above single-center procedure is repeated for every nucleus in the system. The overall scheme is extremely simple in principle and in practice. In Sec. V it is tested on representative diatomic and polyatomic molecules.

V. DIATOMIC AND POLYATOMIC TESTS

The tests reported here are not exhaustive. We simply wish to demonstrate the viability of the present method and to assess the sort of accuracy obtainable. Our first series of tests is performed on *diatomic* systems in order that various integrals of the density functional type may be compared with exact results from our existing numerical diatomic program.[1]

We consider specifically the diatomic systems H_2, N_2, and P_2 at their equilibrium internuclear separations. Furthermore, we choose as test integrands the functionals

$$F(\mathbf{r}) = \rho, \rho^{4/3}, \rho^{5/3}, V_{el}\rho, \quad \text{and} \quad V_{nucl}\rho, \qquad (26)$$

where ρ is the total electron density, V_{el} is the corresponding Coulomb potential, and V_{nucl} is the potential due to the atomic nuclei. The second and third of the above integrands, $\rho^{4/3}$ and $\rho^{5/3}$, are well-known density functional approximations for exchange and kinetic energy densities, respectively, while the final integrands $V_{el}\rho$ and $V_{nucl}\rho$ are components of the potential energy. In the above selection of integrands, therefore, all major components of the total energy of a many-electron system are represented.

For convenience, however, we model the total density ρ simply as a sum of free atomic densities obtained from the Hartree–Fock orbitals of Clementi and Roetti.[31] This approximation simplifies the present tests tremendously, but is not expected to bias our ultimate assessment in any way. Within this model, the value of the potential V_{el} at each of the integration mesh points is calculated analytically.

In diatomic systems, of course, axial symmetry reduces our problem from three dimensions to only two. Full solid-angle integration as described in Sec. IV is therefore unnecessary. We wish, nevertheless, to estimate the potential accuracy of the present integration scheme in general polyatomic situations, and therefore we ignore axial symmetry in these diatomic tests. In Tables I to III, numerical integrals of the five functionals of Eq. (26) are presented for 50-point and for 110-point angular meshes. The associated radial meshes are the same in both cases, with the number of radial points given by the rules of Sec. IV. We observe that an overall accuracy in the order of five or six significant figures is obtained, and that all five integrands, despite their qualitative differences, are equally well treated.

Further results are presented in Table IV for the numerical integration of the total electronic charge in seven polyatomic systems representing a wide variety of typical molecular geometries. Again we assume, for convenience only, that the total molecular charge density is just a sum of atomic Hartree–Fock densities. However, the disposition of the single-center subintegration meshes in polyatomic systems is slightly more complicated than for the previous dimers. This is due to the fact that somewhat finer meshes are required for *central* atoms in polyatomic molecules than for ligand atoms or atoms in linear coordination. We therefore assign roughly twice as many angular points to the central atoms in the molecules of Table IV (except for C in linear CO_2) than are assigned to the ligand atoms. Also, each central atom is assigned ten additional *radial* points as well. These *ad hoc* rules for assigning mesh points are nothing more than rough guides in determining efficient point distributions. They are not rigorously based, nor should they be viewed as corrupting the fundamental simplicity of the present integration scheme.

Results are given in Table IV for two classes of integration meshes, coarse meshes containing 50-point angular components (110 for central atoms) and somewhat finer meshes containing 110-point angular parts (194 for central atoms). The same *radial* meshes are used in either case, in accordance with the rules of Sec. IV and the *ad hoc* addition of ten radial points for central atoms. The resulting charge integrals display a relative accuracy in the order of 10^{-4} in the case of the coarse meshes, and 10^{-5} in the case of the finer meshes. In view of the previous diatomic results, we infer that similar precision would be obtained as well for the other integrands in the list of Eq. (26).

The recent cellular method of Boerrigter *et al.*[13] is of high accuracy also, but the great simplicity of the present scheme and its relatively straightforward extension to solution of Poisson's equation (see Sec. II) are strong advantages. Still higher accuracy may, of course, be achieved by increasing the number of quadrature points even further.

TABLE I. Numerical integration in H_2.

Integrand	Exact	Angular mesh points	
		50	110
ρ	2.000 00	1.999 98	2.000 00
$\rho^{4/3}$	0.660 758	0.660 746	0.660 751
$\rho^{5/3}$	0.257 193	0.257 190	0.257 190
$V_{el}\rho$	2.257 04	2.257 00	2.257 02
$|V_{nucl}\rho|$	3.220 08	3.220 05	3.220 07

TABLE II. Numerical integration in N_2.

Integrand	Exact	Angular mesh points	
		50	110
ρ	14.0001	14.0003	14.0000
$\rho^{4/3}$	15.9961	15.9963	15.9961
$\rho^{5/3}$	34.3728	34.3733	34.3729
$V_{el}\rho$	148.988	148.990	148.988
$|V_{nucl}\rho|$	303.106	303.115	303.109

TABLE III. Numerical integration in P_2.

| Integrand | Exact | Angular mesh points | |
		50	110
ρ	30.0001	29.9993	30.0001
$\rho^{4/3}$	56.3134	56.3143	56.3135
$\rho^{5/3}$	220.002	220.004	220.001
$V_{el}\rho$	737.814	737.818	737.814
$|V_{nucl}\rho|$	1749.64	1749.74	1749.73

Note, however, that extremely high precision is not, in fact, required in calculating most quantities of chemical interest. Chemically interesting quantities, such as dissociation energies, can normally be expressed as *differences* between molecular and atomic data. If, therefore, molecular and atomic reference calculations are performed consistently, then cancellation of numerical errors obviates the need for results of high absolute precision. Cancellation of numerical errors has been very useful in our earlier diatomic work[1] and will no doubt assist our future efforts as well.

VI. CONCLUSIONS

In the present communication, we have addressed the problem of numerical integration in molecular systems by decomposing the integrand into single-center terms, each of which may then be integrated by standard single-center numerical techniques. Our basic decomposition scheme may also be applied to solution of Poisson's equation (work in progress) and eventually, we hope, to the computation of numerical molecular orbitals. This work is only the first step in the development of a comprehensive program system for nonbasis-set quantum chemical calculations. Alternatively, the present scheme may be usefully incorporated into existing density functional LCAO programs such as those of Baerends et al.,[17] Dunlap et al.,[32] etc., all of which rely to some degree on numerical integration techniques.

The tests of Sec. V demonstrate that the present scheme is both accurate and practical. Results of high precision (five or six figures) are obtained with a few thousand integration points per atom. Notice, also, that the necessary number of points may be reduced dramatically in molecules of appro-

TABLE IV. Charge integration in polyatomic systems.

| Molecule | Exact | Angular mesh points | |
		50[a]	110[b]
CO_2	22.0001	22.0004	21.9995
H_2O	10.0000	10.0006	10.0001
BF_3	31.9999	32.0003	32.0003
NH_3	10.0000	10.0013	10.0001
CH_4	10.0000	10.0020	10.0002
PF_5	59.9998	60.0029	59.9986
SF_6	69.9997	70.0051	69.9995

[a] 110 for central atoms, plus 10 additional radial points.
[b] 194 for central atoms, plus 10 additional radial points.

priate geometries if the respective octahedral and icosahedral symmetries of Lebedev's[24-27] and Konyaev's[28] angular point distributions are exploited.

The present results are very encouraging. Further investigations and applications of this novel polyatomic integration scheme will be reported in future communications.

ACKNOWLEDGMENTS

APPENDIX: ATOMIC SIZE ADJUSTMENTS

To simplify the following discussion, the terminology cell "face" or cell "boundary" will be used somewhat loosely. Our fuzzy cells do not, of course, have discrete faces. We shall, however, use these terms to denote the surfaces on which the cutoff functions $s(\mu_{ij})$ take the intermediate value 1/2.

The faces of the Voronoi polyhedra described in Sec. III bisect the internuclear axes exactly. In *heteronuclear* systems, however, variations in atomic size do not necessarily favor such a "democratic" partitioning. We desire, therefore, to shift our cell boundaries away from the internuclear midpoints in heteronuclear molecules.

First of all, we adopt as a definition of atomic size the empirical atomic radii of Bragg and Slater.[30] Bragg–Slater radii are derived from the observation that interatomic bond lengths in solids and molecules, whether ionic or covalent, are approximately equal to pairwise sums of unique atomic radii. This observation may be rationalized by the further observation that these unique atomic radii correlate remarkably well with the positions of valence-shell probability-density maxima obtained independently from theoretical calculations on free atoms. In the present work, Bragg–Slater radii as tabulated in Ref. 30 are therefore used as guides in the adjustment of cell boundaries (and also the adjustment of the radial integration parameters r_m of Sec. IV). For hydrogen, however, we prefer a radius of 0.35 Å, somewhat larger than Slater's value of 0.25 Å. Details of the boundary adjustment procedure are now outlined.

A cell boundary is defined by the surface on which the cutoff function $s(\mu_{ij})$ has value 1/2, or, equivalently, the surface on which its argument μ_{ij} has value 0. As emphasized in Sec. III, the surfaces $\mu_{ij} = 0$ are perpendicular bisectors of internuclear axes, and thus the faces of the cells discussed so far lie exactly at internuclear midpoints. Our cell boundaries can be shifted *off center*, however, by a simple transformation of coordinates from μ_{ij} to a new coordinate v_{ij}. In other words, a heteronuclear cutoff profile $s_{het}(\mu_{ij})$ can be defined in the following manner:

$$s_{het}(\mu_{ij}) = s(v_{ij}), \tag{A1}$$

where the new argument v_{ij} is related, in the present work, to the old argument μ_{ij} by

$$v_{ij} = \mu_{ij} + a_{ij}(1 - \mu_{ij}^2) \tag{A2}$$

and where a_{ij} is a parameter with value in the range

$$|a_{ij}| \leqslant \tfrac{1}{2} \tag{A3}$$

to ensure monotonicity. We thus transform our cell boundaries from bisecting planes to hyperboloidal surfaces $v_{ij} = 0$, towards center i or towards center j depending on the sign of a_{ij}. Though other transformations are also conceivable, Eq. (A2) is particularly simple.

The above transformation is easily incorporated into the cell-construction algorithm of Sec. III. We simply require for each nuclear pair i and j, with respective Bragg–Slater radii R_i and R_j and internuclear separation R_{ij}, a value for parameter a_{ij}. In order to specify a_{ij}, consider the point at which the internuclear ij axis intersects the *shifted* boundary surface $v_{ij} = 0$, and let us *assume* that the ratio of r_i to r_j (the distances to the respective nuclei) is equal to the *ratio of the Bragg–Slater radii*:

$$\frac{r_i}{r_j} = \frac{R_i}{R_j} \equiv \chi. \tag{A4}$$

Parameter a_{ij} is then determined by the condition $v_{ij} = 0$ as follows:

$$a_{ij} = \frac{u_{ij}}{u_{ij}^2 - 1}, \tag{A5}$$

where u_{ij} is related to the ratio χ of the Bragg–Slater radii by

$$u_{ij} = \frac{r_i - r_j}{R_{ij}} = \frac{r_i - r_j}{r_i + r_j} = \frac{\chi - 1}{\chi + 1}. \tag{A6}$$

Should, however, the resulting a_{ij} fall outside the range allowed by Eq. (A3), then we simply assign the appropriate endpoint value $\pm 1/2$. This occurs if the Bragg–Slater radii R_i and R_j differ by a factor greater than roughly 2.4. The transformation of Eq. (A2) does not, therefore, provide unlimited freedom in shifting cell boundaries, but the available flexibility is apparently quite adequate.

The adjusted partitioning scheme described in this section gives significantly better results than obtained from "homonuclear" decompositions. All of the polyatomic integrals discussed in Sec. V have therefore been calculated using shifted cell boundaries.

[1] A. D. Becke, Ph.D. dissertation, McMaster University, Hamilton, Canada (1981); J. Chem. Phys. **76**, 6037 (1982); **78**, 4787 (1983).

[2] J. C. Slater, *The Self-Consistent Field for Molecules and Solids* (McGraw-Hill, New York, 1974).

[3] A. D. Becke, Phys. Rev. A **33**, 2786 (1986).

[4] A. D. Becke, J. Chem. Phys. **84**, 4524 (1986).

[5] L. Laaksonen, D. Sundholm, and P. Pyykkö, Int. J. Quantum Chem. **27**, 601 (1985).

[6] L. Laaksonen, P. Pyykkö, and D. Sundholm, Comput. Phys. Rep. **4**, 315 (1986).

[7] S. A. Alexander and H. J. Monkhorst, Int. J. Quantum Chem. **32**, 361 (1987).

[8] T. Ziegler, V. Tschinke, and A. Becke, J. Am. Chem. Soc. **109**, 1351 (1987).

[9] T. Ziegler, V. Tschinke, and A. Becke, Polyhedron **6**, 685 (1987).

[10] *Local Density Approximations in Quantum Chemistry and Solid State Physics*, edited by J. P. Dahl and J. Avery (Plenum, New York, 1984); *Density Functional Methods in Physics*, edited by R. M. Dreizler and J. da Providencia (Plenum, New York, 1985); *Density Matrices and Density Functionals*, edited by R. Erdahl and V. H. Smith, Jr. (Reidel, Dordrecht, 1987).

[11] K. Lee, J. Callaway, and S. Dhar, Phys. Rev. B **30**, 1724 (1984); S. Dhar, A. Ziegler, D. G. Kanhere, and J. Callaway, J. Chem. Phys. **82**, 868 (1985).

[12] G. B. Arfken, *Mathematical Methods for Physicists*, 2nd ed. (Academic, New York, 1970).

[13] P. M. Boerrigter, G. te Velde, and E. J. Baerends, Int. J. Quantum Chem. (to be published).

[14] R. F. W. Bader and T. T. Nguyen-Dang, Adv. Quantum Chem. **14**, 63 (1981).

[15] F. W. Biegler-Koenig, T. T. Nguyen-Dang, Y. Tal, R. F. W. Bader, and A. J. Duke, J. Phys. B **14**, 2739 (1981); F. W. Biegler-Koenig, R. F. W. Bader, and Ting-Hua Tang, J. Comput. Chem. **3**, 317 (1982).

[16] D. E. Ellis, Int. J. Quantum Chem. Quantum Chem. Symp. **2**, 35 (1968); D. E. Ellis and G. S. Painter, Phys. Rev. B **2**, 2887 (1970).

[17] E. J. Baerends and P. Ros, Int. J. Quantum Chem. Quantum Chem. Symp. **12**, 169 (1978).

[18] C. B. Haselgrove, Math. Comput. **15**, 323 (1961); H. Conroy, J. Chem. Phys. **47**, 5307 (1967).

[19] S. F. Boys and P. Rajagopal, Adv. Quantum Chem. **2**, 1 (1965).

[20] N. N. Medvedev, J. Comput. Phys. **67**, 223 (1986).

[21] A. D. McLaren, Math. Comput. **17**, 361 (1963).

[22] A. H. Stroud, *Approximate Calculation of Multiple Integrals* (Prentice-Hall, Englewood Cliffs, 1971).

[23] S. L. Sobolev, Sibirsk. Mat. Zh. **3**, 769 (1962). References 23 to 28 are in Russian. English translations are available in Siberian Math. J. (Sibirsk. Mat. Zh.), U.S.S.R. Comput. Math. and Math. Phys. (Zh. Vychisl. Mat. Mat. Fiz.), and Math. Notes (Mat. Zametki).

[24] V. I. Lebedev, Zh. Vychisl. Mat. Mat. Fiz. **15**, 48 (1975), also note erratum in Ref. 25.

[25] V. I. Lebedev, Zh. Vychisl. Mat. Mat. Fiz. **16**, 293 (1976).

[26] V. I. Lebedev, Sibirsk. Mat. Zh. **18**, 132 (1977).

[27] V. I. Lebedev, *Proc. Conf. Novosibirsk (1978)*, edited by S. L. Sobolev (Nauka Sibirsk. Otdel., Novosibirsk, 1980).

[28] S. I. Konyaev, Mat. Zametki **25**, 629 (1979).

[29] *Handbook of Mathematical Functions*, edited by M. Abramowitz and I. A. Stegun (Dover, New York, 1970).

[30] J. C. Slater, J. Chem. Phys. **41**, 3199 (1964); J. C. Slater, *Quantum Theory of Molecules and Solids* (McGraw-Hill, New York, 1965), Vol. 2.

[31] E. Clementi and C. Roetti, At. Data Nucl. Data Tables **14**, 177 (1974).

[32] B. I. Dunlap, J. W. D. Connolly, and J. R. Sabin, J. Chem. Phys. **71**, 3396, 4993 (1979).